Available online at website: https://journal.bcrec.id/index.php/bcrec

Bulletin of Chemical Reaction Engineering & Catalysis, 21 (1) 2026, 11-21

Original Research Article

Tailoring Photocatalytic Activity of Sol-Gel-Derived Bismuth Oxide via Calcination Time Optimization for Methyl Orange Degradation

Yayuk Astuti*, Agus Muslim, Adi Darmawan

Chemistry Department, Faculty of Sciences and Mathematics, Universitas Diponegoro, Jl. Prof. Jacob Rais, Tembalang, Semarang, 50275, Indonesia.

Received: 25th July 2025; Revised: 28th October 2025; Accepted: 29th October 2025
Available online: 6th November 2025; Published regularly: April 2026

Abstract

Bismuth oxide (Bi_2O_3) is a yellow solid, has good electrical properties and a wide band gap energy (2-3.96 eV). Therefore, this material is commonly used as a photocatalyst. This study aims to synthesize bismuth oxide using the sol-gel method, determine its physicochemical characteristics and photocatalytic activity in the degradation of methyl orange dyes. Bi_2O_3 is synthesized from $Bi(NO_3)_3.5H_2O$ which is reacted with citric acid at 100 ° C for 20 hours. The formed gel is then dried and calcined at 600 °C for 1, 2, 3, 4 and 5 hours. The synthesis results in the form of pale-yellow powder with the same crystal system that is a mixture of α-Bi_2O_3 (monoclinic) and γ-Bi_2O_3 (BCC) and has almost the same morphology that is similar to coral and has a particle size of 1-8 µm. The results of photocatalytic activity tests showed that the constant rate of degradation reaction of methyl orange by bismuth oxide with calcination time of 1, 2, 3, 4, and 5 hours respectively was 2.76×10^{-5} s^{-1}, 2.65×10^{-5} s^{-1}, 2.53×10^{-5} s^{-1}, 2.81×10^{-5} s^{-1} and 3.87×10^{-5} s^{-1}. Bismuth oxide with a calcination time of 5 hours has the highest photocatalytic activity. Meanwhile, bismuth oxide with a calcination time of 5 hours has a band-gap of 2.86 eV and 2.64 eV. The stages of decomposition of bismuth oxide material with a calcination time of 5 hours consisted of 3 release stages namely H_2O, CO_2, $C_xH_yO_z$ respectively 12.20%, 5.33% 30.54%.

Keywords: Bismuth oxide; Sol-gel; Calcination variation; Photocatalyst; Methyl orange

How to Cite: Astuti, Y., Muslim, A., Darmawan, A. (2025). Tailoring Photocatalytic Activity of Sol-Gel-Derived Bismuth Oxide via Calcination Time Optimization for Methyl Orange Degradation. *Bulletin of Chemical Reaction Engineering & Catalysis*, 21 (1), 11-21. (doi: 10.9767/bcrec.20452)

Permalink/DOI: https://doi.org/10.9767/bcrec.20452

1. Introduction

Bismuth Oxide (Bi_2O_3) is a semiconductor with the physical form of pale-yellow powder material [1], non-toxic, non-carcinogenic and widely applied as a photocatalyst [2–5]. Similar to other widely studied metal oxide photocatalysts such as titanium dioxide (TiO_2) [6,7] and zinc oxide (ZnO) [8,9], Bi_2O_3 exhibits strong photocatalytic activity due to its suitable electronic structure and high photochemical stability. However, unlike TiO_2 and ZnO, which possess relatively wide band gaps of approximately 3.0–3.2 eV and 3.2–3.3 eV, respectively, Bi_2O_3 has a narrower band gap ranging from 2.0 to 3.96 eV [10]. This narrower band gap enables Bi_2O_3 to absorb visible light more effectively, thereby enhancing its potential for photocatalytic applications under solar irradiation.

Bismuth oxide can be synthesized by several methods, including deposition method [11], solution combustion method [12–16], sol-gel method [17], and the hydrothermal method [18]. Among these methods, the sol-gel method has several advantages, including high purity, high degree of homogeneity because the reagents are mixed at the molecular level, synthesis at low temperatures because certain materials can be carried out at room temperature [19], the degree of thermal stability good, high mechanical

* Corresponding Author.
Email: yayuk.astuti@live.undip.ac.id (Y. Astuti)

stability, no reaction with residual compounds and loss of material due to evaporation can be reduced [20]. The stages of the sol-gel process include the first stage of hydrolysis, the second stage of condensation, the third stage of maturation (aging) and the fourth stage of drying. Factors affecting the sol-gel method include calcination temperature. Calcination temperature and calcination duration have a significant effect on the crystallinity, surface structure of the synthesis product [21]. These properties will affect the application of bismuth oxide.

Research conducted by Astuti *et al*. [22] shows that variations in calcination temperature in the sol-gel method affect the particle size and photocatalytic activity of Bi_2O_3. Similar results were also found by Ilsatoham *et al*. [23], who reported that variations in substrate temperature in the production of thin Bi_2O_3 layers using the sol-gel spray coating method can change the crystal phase and morphology of the material. Meanwhile, research conducted by Kusworo *et al*. [24] shows that the application of the sol-gel method in the developmenst of metal oxide-based catalytic composite membranes can produce a material structure that is homogeneous, thermally stable, and has high mechanical durability. These findings reinforce that the sol-gel method is an effective and versatile synthesis technique for producing high-performance oxide materials, including in the development of bismuth oxide and other functional materials.

Synthesis of bismuth oxide by the sol-gel method has been carried out by Mallahi *et al*. [1] at calcination temperatures of 200 ^oC, 500 ^oC, 800 ^oC with a precursor ratio (bismuth nitrate pentahydrate: citric acid) 1: 1. At this temperature variation the crystal has a form of pseudospherical morphology and when the calcination temperature is raised to 800 °C the particles form microspheroid and agglomerate. In this study, bismuth oxide photocatalyst activity synthesized and band gap values were not explored / determined.

Astuti [22] has synthesized bismuth oxide using the sol-gel method with a precursor ratio of 1:1 and calcination temperature variations of 500 °C, 600 °C and 700 °C as well as determining fotakalis activity to degrade methyl orange. The results of this synthesis produce yellow powder with the best photocatalytic activity at a temperature of 700 °C which is 5.69×10^{-5} s^{-1}. Besides that, Astuti [25] has synthesized bismuth oxide using the sol-gel method with a precursor ratio of 1:2 at calcination temperature of 700 °C and determined the photocatalyst activity to degrade methyl orange. The synthesis results in the form of pale-yellow powder with the percentage of methyl orange degradation 46.28%. In terms of calcination time impact, Hwang *et al*. [26] have conducted research on the effect of Al-substitution on the stability of the $LiMn_2O_4$ spinel synthesized using the sol-gel method with citric acid precursors with variations in calcination time of 10, 15 and 20 hours at 800 °C. SEM and TEM results show that the particle size is greater with increasing calcination time and shows good and uniform crystallinity and particle agglomeration increases.

Based on the above background, it is necessary to develop bismuth oxide synthesis to get high photocatalyst activity values using the sol-gel method through calcination time variation. Therefore, this study aims to synthesize bismuth oxide using the sol-gel method with calcination time variations of 1, 2, 3, 4 and 5 hours at 600 °C with a precursor ratio of 1:2, determining the character of the synthesis results obtained for identify the crystal structure, surface morphology, band-gap, functional groups contained in the synthesized material, decomposition of the material during the calcination process using XRD, SEM, DRS-UV, FTIR and TGA and determine the photocatalytic activity of the synthesis results for the degradation of methyl orange dyes.

2. Materials and Method

2.1 Materials

The materials used in this study include $Bi(NO_3)_3.5H_2O$ from SIGMA-ALDRICH, 65% HNO3, citric acid monohydrate, PEG 6000, and methyl orange from MERCK, distilled water.

2.2 Bismuth Oxide Synthesis

The synthesis of Bismuth oxide by the sol-gel method follows the method presented by Mallahi *et al*. [1] with a slight modification. 4 grams of $Bi(NO_3)_3.5H_2O$ were mixed with citric acid at a molar ratio of 1:2 and dissolved in a 50 mL nitric acid solution with 1 gram of PEG 6000 added. Furthermore, the solution was heated at 100 °C for 20 hours at a moderate speed of 667 rpm. Cooling solution or aging process was conducted for 12 hours. The formed gel was then dried in an oven (Thermo Scientific F47910-33) at 100 °C for 12 hours and continued with calcination in the furnace (Eurotherm 2116) at 600 ° C for 1, 2, 3, 4 and 5 hours.

2.3 Photocatalytic Activity Test

The photocatalyst activity test was carried out in a photocatalyst reactor, the working solution used for the photocatalyst activity test was 5 ppm methyl orange solution. 0.1 grams of bismuth oxide as the result of synthesis were put into 50 mL of working solution, then the mixing process was carried out at medium speed (667 rpm). The stirring process was carried out for 2 hours for the photocatalyst test without light,

while the photocatalyst test used UV-a (352 nm) with 15 watt of power used time variations of 2, 4, 6, 8, and 10 hours. Then proceed with the process of reading the absorbance of the samples of each variation and wavelength using UV-Vis spectroscopy.

2.4 Characterizations

The powder obtained from bismuth oxide synthesis with calcination time variation of 1, 2, 3, 4 and 5 hours were each characterized using XRD (Shimadzu 7000) (Cu-Kα light source which has a wave of 1.54178 Å and a voltage of 30.0 kV, electric current 30 mA) and FTIR (Shimadzu Iraffinity-1) in the range of wave numbers 500-4500 cm^{-1}. The morphology of the bismuth oxide synthesized was analyzed using SEM type JEOL 6510 LA instruments in the energy range of 0-20 keV voltage of 20.0 kV calculated speed of 2729 cps with magnifications of 1000 and 5000 times. Determination of the band-gap of bismuth oxide synthesized used the Touc Plot method with UV 1700 Pharmaspec DRS-UV type instruments. Analysis of the decomposition of the bismuth oxide material synthesized used the LGASEIS STA Platinum Series TGA instrument with Crucible Alumina at a temperature of 30-700 ^oC with a heat flow of 5 ^oC per minute.

3. Results and Discussion

3.1 Synthesis Products

Figure 1 shows the synthesized products obtained from varying calcination times under the same temperature. The synthesized products after calcination exhibit a similar trend in color but differing masses with products calcined for 1, 2, 3, 4 and 5 hours at 2.65, 2.11, 1.88, 1.63 and 1.44 grams, respectively. The yellow-colored powder in all samples indicates that bismuth oxide has successfully been formed as in accordance with the statement of [27] that bismuth oxide appears as yellow powder. The color, its intrinsic optical property, is produced by the adsorption of visible light in the wavelength range of 400 to 700 nm. A semiconductor material will absorb light that has shorter wavelengths or a band-gap energy between 2.0-3.31 eV. This means that bismuth oxide can absorb lights with greater energy, including the blue and violet lights (2.5-3.0 eV). The absorbed blue and violet lights are interpreted by the naked eyes as the color yellow possessed by the material of interest (Richerson, 2005). The different mass weights obtained are dependant upon the calcination time; longer calcination time results in lower weight of the synthesized powder.

3.2 Crystal Structure

XRD diffractograms of the bismuth oxides produced at varying calcination times can be seen in Figure 2. Characterization with XRD was done by comparing the measured peaks of the samples with peaks from the JCPDS database for α-Bi_2O_3 (41-1449), β-Bi_2O_3 (27-0050), γ-Bi_2O_3 (45-1344), and ω-Bi_2O_3 (50-1088).

Bismuth oxide synthesized with calcination times of 1, 2, 3, 4 and 5 hours has the same mixed crystal structure of α-Bi_2O_3 (monoclinic) and γ-Bi_2O_3 (body center cubic). The α-Bi_2O_3 species is crystallized into a monoclinic system with a = 5.8499, b = 8.1698, and c = 7.5123 linear parameters. Its angular parameters are $\alpha = 90^0$, $\beta = 112.988^0$ and $\gamma = 90^0$. The γ-Bi_2O_3 species is crystallized into a body center cubic system with a = 10.86 linear parameter. Its angular parameters were $\alpha = 90^0$, $\beta = 90^0$, and $\gamma = 90^0$. Data on the

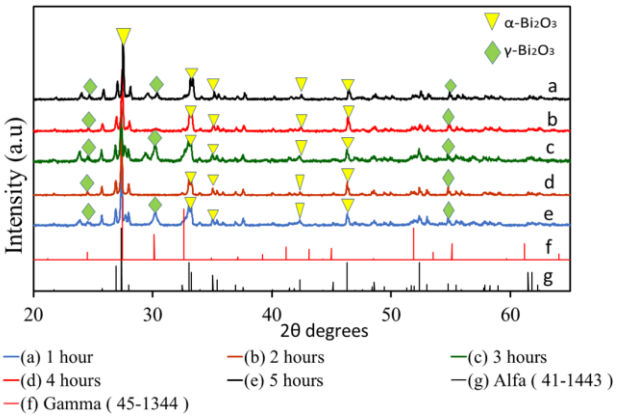

Figure 2. XRD results for calcination time variations of 1,2,3,4 and 5 hours and the JCPDS database No.14-1449 comparison.

Figure 1. The synthesized bismuth oxide powders: (a). 1 hour of calcination, (b). 2 hours of calcination, (c). 3 hours of calcination, (d). 4 hours of calcination, e. 5 hours of calcination.

three highest (most intense) 2θ values of the bismuth oxides are shown in Table 1. These data are in accordance with the JCPDS database numbers 41-1449 for α-Bi_2O_3 and 45-1344 for the γ-Bi_2O_3.

3.3 Product Morphology

Identification of the morphological shapes of the bismuth oxide crystals formed were carried out using SEM by looking at the differences in morphological images of the synthesized compound. Figure 3 displays the results of SEM imaging of the synthesized bismuth oxide via sol-gel method at 600 °C. SEM results show that the 5000x magnified morphology of the bismuth oxide synthesized using the sol-gel method has an irregular and non-uniform shape with cavities on the surface of the crystal with sizes around 1-8 µm.

3.4 Bismuth Oxide Compound Confirmation Through Functional Group Identification

The bismuth oxide samples synthesized were analyzed by FTIR spectrophotometer to identify the functional groups contained in the sample through identifications of wavelengths produced in the spectra. FTIR spectra of the synthesized bismuth oxide via the sol-gel method at different calcination times are shown in Figure 4. The synthesized bismuth oxide infrared spectra are shown in Figure 4. The results of the FTIR analysis on the synthesized bismuth oxide present that the five samples, namely bismuth oxides with calcination time variations of 1, 2, 3, 4 and 5 hours, have a peak absorption at a wavenumber of about 844 cm^{-1} indicating the presence of Bi-O-Bi group [28] in the synthesized products. The Bi-O-Bi grup is a strong indication of the presence of Bi_2O_3 in the synthesized product. In addition, all five samples possess wide and sharp absorption peak at around 1384 cm^{-1} signifying the existence of Bi-O stretching vibration [29]. Although some references mention the presence of NO_3 in this absorption band [30], EDX characterization of Figure 5 demonstrate that the N element was non-existent. Moreover, the intense peak ought not to only indicate NO_3, since the existence of only NO_3 implies that there is very little formation of Bi_2O_3. Proven not to be the case, the authors conclude that the peak at that wavenumber denotes Bi-O.

3.5 Material Decomposition during Calcination Process

Changes that occur during the calcination process can be known using a thermogravimetric tool by calculating the change in mass due to a gradual increase in temperature. The obtained synthesized product with differing calcination

Table 1. XRD 2θ data of the synthesized

Calcination Time	Crystal Structure (2θ)	
	α-Bi_2O_3	γ-Bi_2O_3
1 hour	27.374	24.731
	33.905	30.515
	46.326	50.211
2 hours	27.411	24.687
	33.255	40.144
	46.334	50.251
3 hours	27.352	24.684
	33.119	30.459
	46.391	50.231
4 hours	27.382	24.595
	33.219	30.466
	46.312	50.213
5 hours	27.549	24.614
	33.393	30.487
	46.459	50.242

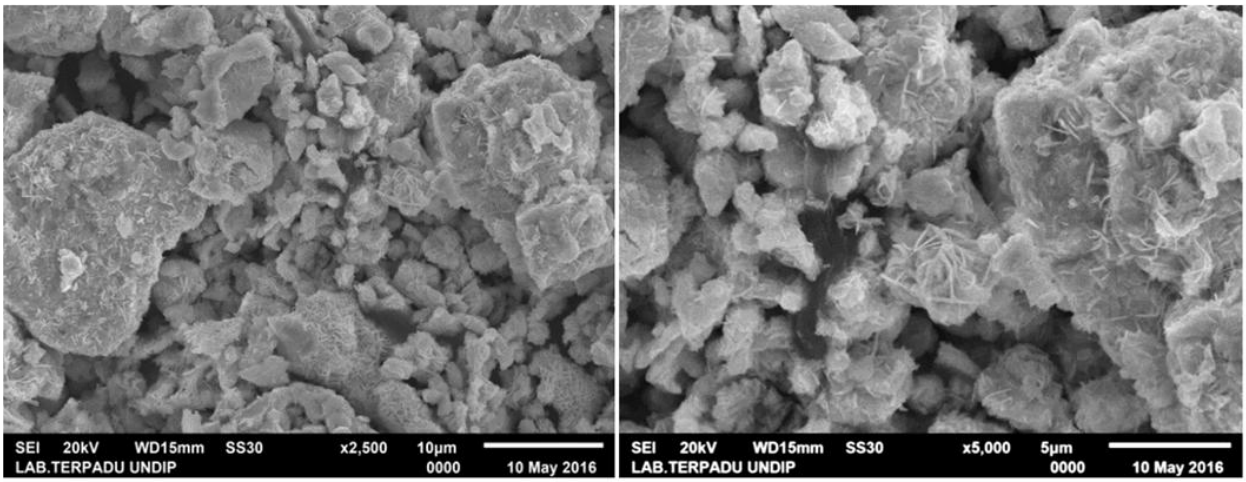

Figure 3. SEM images of bismuth oxide synthesized with 5 hours calcination time under 2500x and 5000x magnification.

times are in fundamental the same for all 1, 2, 3, 4 or 5 hours calcination time. Thus, the sample analyzed is the bismuth oxide sample calcined for 5 hours at a temperature of 600 ^{0}C that had been dried but had not been calcined.

TGA-DSC curves presented in Figure 6 depict the decomposition that occurs in the uncalcined bismuth oxide compound which can be identified from its change in mass (%) with increasing temperature (^{0}C). The curves obtained are of the multistage decomposition curve. Figure 7 shows the DTG curve showing the change in material mass that occured in three stages. The first stage is the H_2O release or loss of water content still present shown by the sharp TGA graph and the absence of DSC peaks through the endothermal

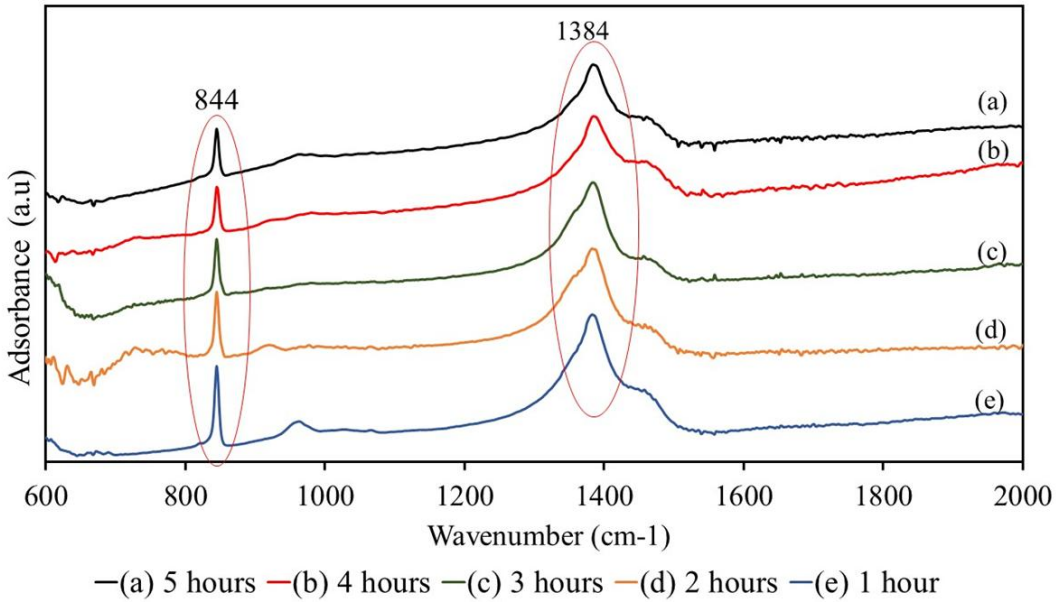

Figure 4. FTIR spectroscopy of the synthesis products with calcination times of 1, 2, 3, 4 and 5 hours.

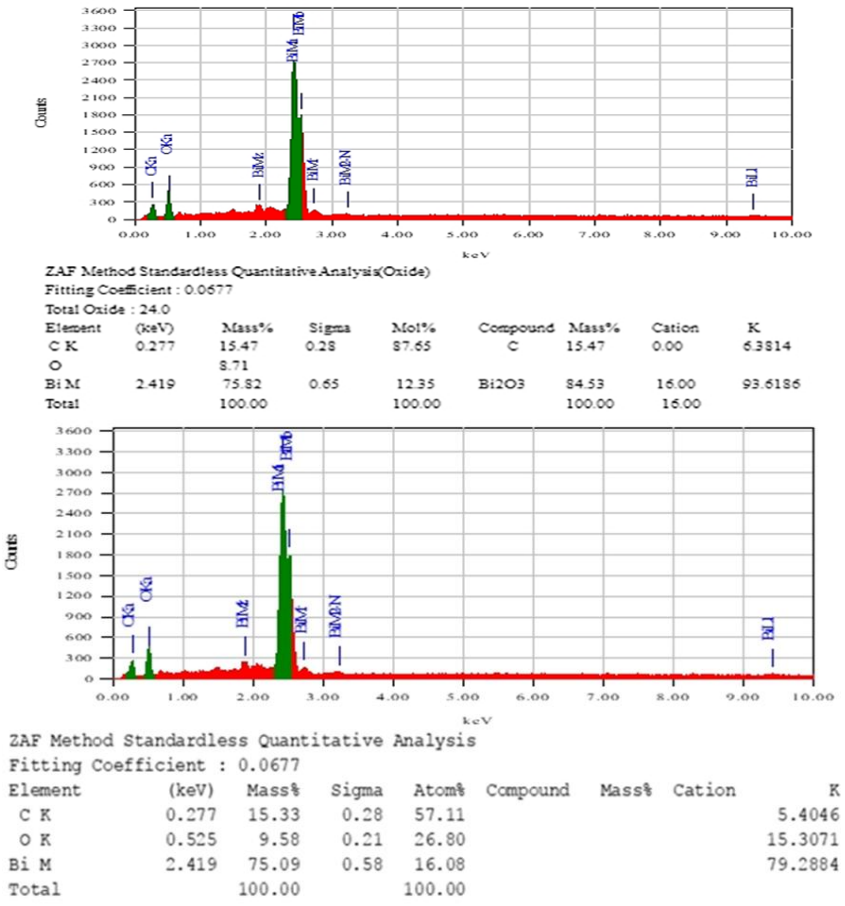

Figure 5. The Bi_2O_3 EDX results for (a) measured sample and (b) pure substance.

process at temperature 40-140 ^{0}C accompanied by a decrease in mass of 12.20%. The second stage is the CO release which is illustrated through a decline in the TGA graph along with the DSC graph with an exothermic process at a temperature of 160-190 ^{0}C accompanied by a decrease in mass of 5.33%. The third stage is assumed to be an implementation of the release of the $C_xH_yO_z$ molecule illustrated by a decline in the TGA graph and exothermic process at 220-340 °C in the DSC graph accompanied by a 30.54% mass loss. At a temperature of 350-440 ^{0}C, the sample did not experience a decrease in mass shown by constant TGA and DSC exothermic graphs. This indicates that the remaining sample is stable Bi_2O_3 with relative mass of 48.07%. The decomposition stages of the material are presented in Table 2.

3.6 Band-Gap Values of 5 Hours Calcination Product

Band-gap values can be determined using the UV-Vis DRS Spectrophotometry. The best sample produced is the sample synthesized with a

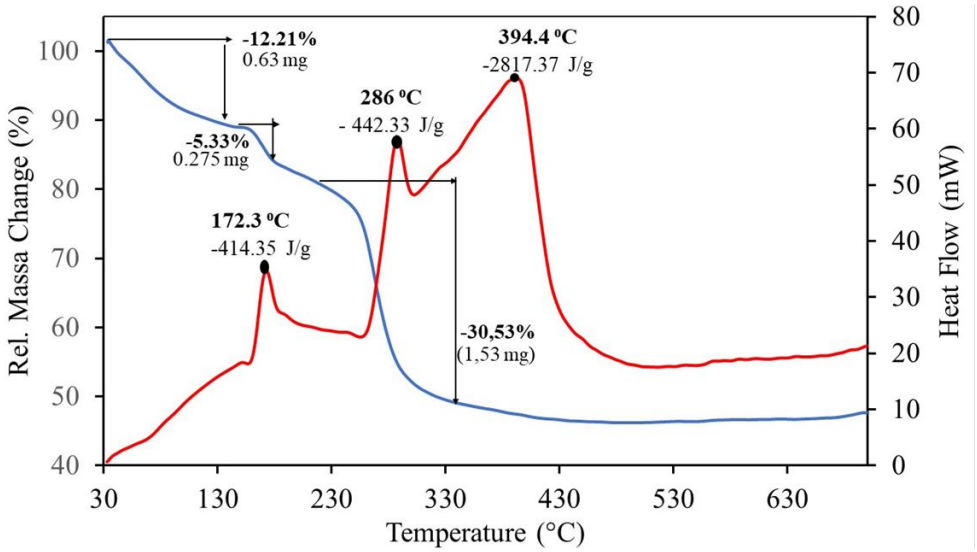

Figure 6. TGA and DSC produced by synthesised bismuth oxide.

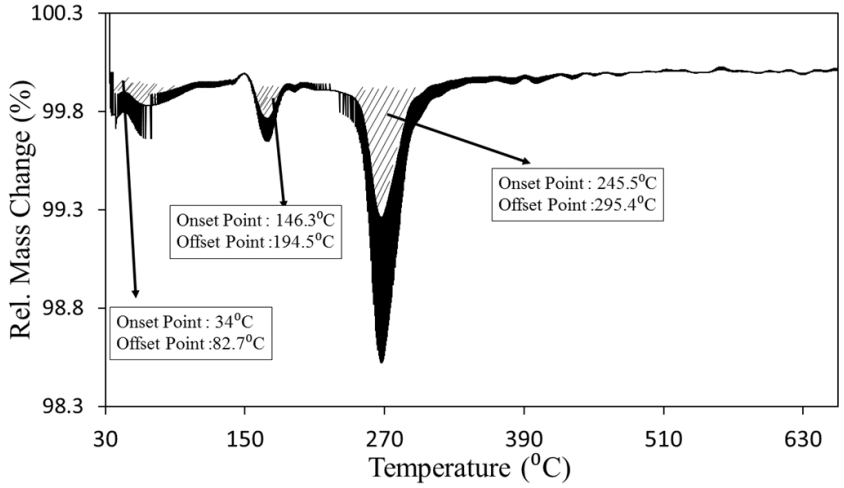

Figure 7. DTG curve of the synthesized bismuth oxide.

Table 2. DSC for the value of ΔH and the reduction in mass of the Bi_2O_3 synthesized using the sol-gel method.

Stages of material decomposition	ΔH (J/g)	Change in relative mass (%)	Temperature of decomposition (°C)
H_2O	414.35	12.21	40-140
CO_2	442.33	5.33	160-190
$C_xH_yO_z$	2817.37	30.53	220-340

calcination time of 5 hours. It was measured for its band-gap values by processing the reflectance data obtained from measurements at wavelengths of 200-800 nm starting from ultraviolet light to visible light.

Figure 8 shows that the absorbance region of the synthesized Bi_2O_3 is within the wavelengths of 200-800 nm. The band-gap value is obtained from the Tauc Plot calculation method by graphing the relationship between hv and $(ahv)^{1/n}$ through drawing a straight line that is tangent to the turning point on the curve to intersect the energy axis. The x-axis is the band gap (E_g) in eV units, while the y-axis is the value of $(ahv)^{1/n}$. This calculation is based on the Tauc Plot equation as follows:

$$(\alpha h\nu)^{\frac{1}{n}} = A(h\nu - E_g) \quad (1)$$

with h = Planck's constant (6.626×10^{-34} J), υ = frequency, E_g = band-gap, A = constant of proporsionality, and n = exponent value indicating the nature of the sample transition [31].

The lines that intersect the x-axis show the band-gap values of the synthesized bismuth oxide. Based on Figure 8, it can be seen that the best synthesized bismuth oxide has two band-gap values of 2.64 eV and 2.86 eV. Bi_2O_3 with a calcination time of 5 hours has two band-gap values because it has a mixed crystal system, enabling it to have more than one band-gap value. This reinforces the reason that bismuth oxide synthesized with 5 hours calcination time has a domininant monoclinic crystal system (α-Bi_2O_3) compared to other crystal structures within the sample, where α-Bi_2O_3 has a band gap value of 2.85 eV. In addition, a band gap value of 2.64 eV also supports the reason for the presence of a cubic crystal system (γ-Bi_2O_3) in bismuth oxide synthesized, where γ- Bi_2O_3 has a band gap of 2.7 eV [32]. This is consistent with the results of the XRD analysis in Section 3.2 which concluded that the crystal structure formed was a mixture of α-Bi_2O_3 and γ- Bi_2O_3 according to JCPDS 41-1443 for α-Bi_2O_3 and JCPDS 45-1344 for γ-Bi_2O_3.

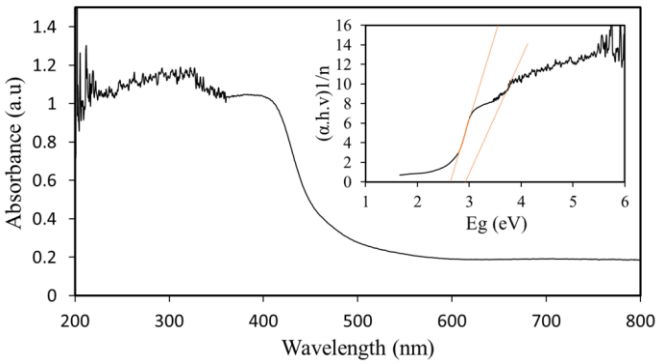

Figure 8. Absorbance vs. wavelength graph of 5 hours calcined Bi_2O_3 product.

3.7 Photocatalyctic Activity

There are three main stages in the photocatalytic reaction, namely: (i) photon absorption by the photocatalytic material, (ii) the formation of e^- and h^+ pairs, and (iii) the formation of hydroxyl radicals (OH·) and superoxide anions ($O_2^{\cdot-}$) as represented in Figure 9 (adopted from Ibhadon & Fitzpatrick [33], Devi *et al.* [34] and Radini *et al.* [35] with modification. The surface of the photocatalyst contains adsorbed water. When light irradiates the photocatalyst, electrons in the photocatalyst move from the valence band (vb) to the conduction band (cb), leaving positive holes in

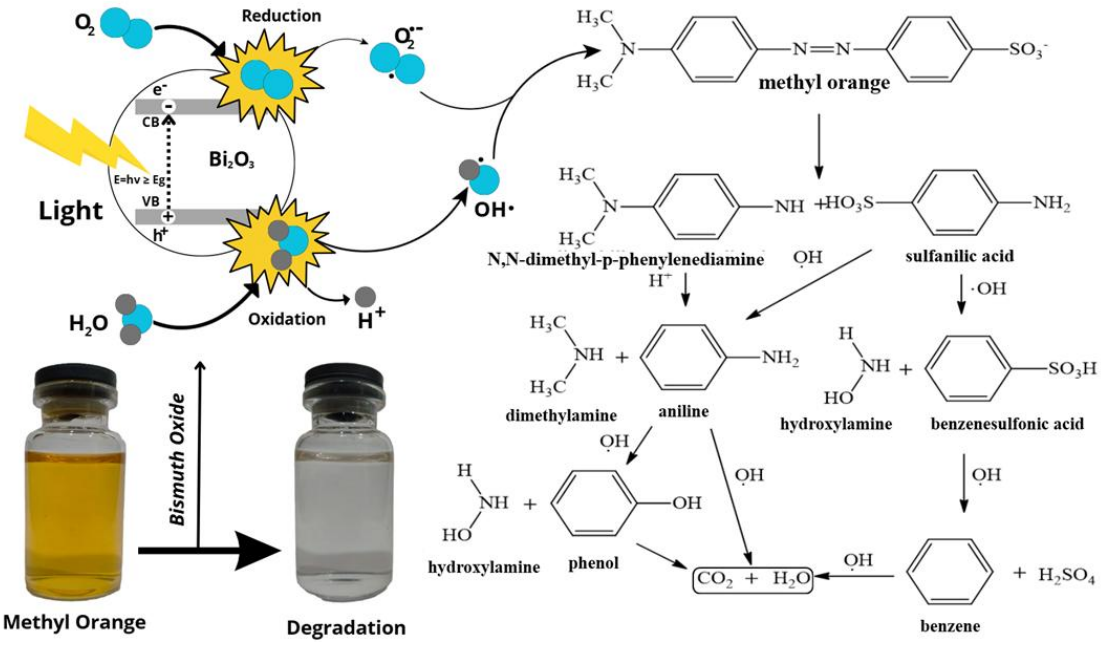

Figure 9. Expected reaction scheme of the methyl orange degradation.

the valence band. These positive holes oxidize the adsorbed water, forming highly reactive hydroxyl radicals. The •OH radical and superoxide ion (O_2•-) in the degradation of methyl orange dye using bismuth oxide photocatalyst can be written as follows [36]:

$Bi_2O_3 + h\upsilon \rightarrow Bi_2O_3(e^-_{(cb)} + h^+_{(vb)})$ (2)

$^{\cdot}OH + h^+_{(vb)} \rightarrow$ •OH (3)

$O_2 + e^-_{(cb)} \rightarrow$ •O_2^- (4)

•O_2^- + $H^+ \rightarrow HO_2$• (5)

$2HO_2$• $\rightarrow O_2 + H_2O_2$ (6)

H_2O_2 + •O_2^- → •OH + OH^- + O_2 (7)

Metil oranye + •OH + •O_2^- → $CO_2 + H_2O +$ H_2SO_4 + NH_2OH + Bi_2O (8)

As shown in Figure 10, the degradation efficiency of methyl orange using the synthesized bismuth oxide prepared via the sol-gel method increased with both calcination times and photocatalysis duration. This improvement can be attributed to enhanced photon absorption and the more efficient generation of charge carriers and reactive species on the photocatalyst surface, which collectively promote the degradation process. It can be seen that the percentages of MO degradation after 2 hours without light for bismuth oxides with calcination times of 1, 2, 3, 4 and 5 hours were 0.28%, 0.28%, 2.81%, 0.28, 0.84%, respectively. Meanwhile, the percentages of MO degradation after the 2 hours photocatalysis process with light on the bismuth oxides synthesized with calcination times of 1, 2, 3, 4 and 5 hours were respectively 2.53%, 0.56%, 6.76%, 3.09%, and 12.67%. The percentages of MO degradation after 4 hours photocatalysis process with light on the bismuth oxides synthesized with calcination time of 1, 2, 3, 4 and 5 hours were 29.57%, 9.57%, 16.62%, 4.78%, and 18.59%. The MO degradations after the 6 hours photocatalysis process with light using the synthesized bismuth oxides with calcination times of 1, 2, 3, 4 and 5 hours were 39.43%, 39.15%, 41.4%, 16.34%, and 52.4%. Degradations of MO after the 8 hours photocatalysis process with light using the synthesized bismuth oxides with calcination times of 1, 2, 3, 4 and 5 hours were 60.28%, 49.57%, 44.22%, 27.04%, and 61.13%. The percentages of MO degradation after the 10 hours photocatalysis process with samples of 1, 2, 3, 4, and 5 hours calcination times were 61.12%, 57.74%, 60.01%, 63.66%, and 74.93%. The sample with calcination time of 5 hours has the best photocatalytic activity demonstrated by having the highest percentage of MO degradation.

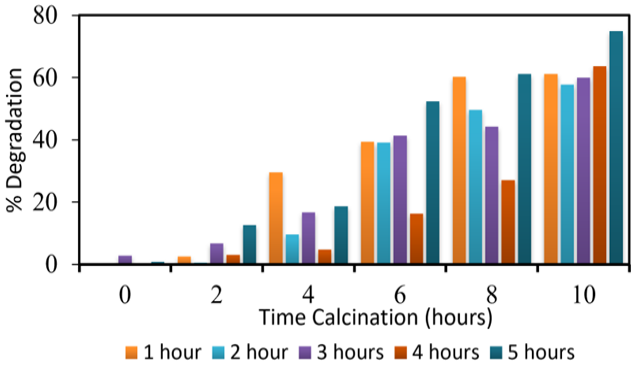

Figure 10. MO degradation for each calcination time variable.

Bi_2O_3 photocatalytic activity against MO can be used to determine the rate of degradation through chemical kinetics. According to Wang [37], dye degradation reactions generally follow the kinetics of the first-order reactions expressed by:

$$\ln C_t = \ln C_o - kt \quad (9)$$

with k = rate constant in the first order (s^{-1}), C_o = initial concentration of methyl orange solution (ppm), and C_t = concentration of methyl orange solution (ppm) at time t. This was also proved by comparing the linear regression graph of first-order and second-order reactions to the degradation of MO by Bi_2O_3 (5 hours). The results show that the first-order reaction kinetics graph is more linear than the second-order reaction kinetics graph, as shown in Figure 11. A graph of the first-order reaction on the degradation of methyl orange dyes by the synthesized bismuth oxide is shown in Figure 11. The slope value of the linear equation obtained on the graph shows the value of the methyl orange degradation rate

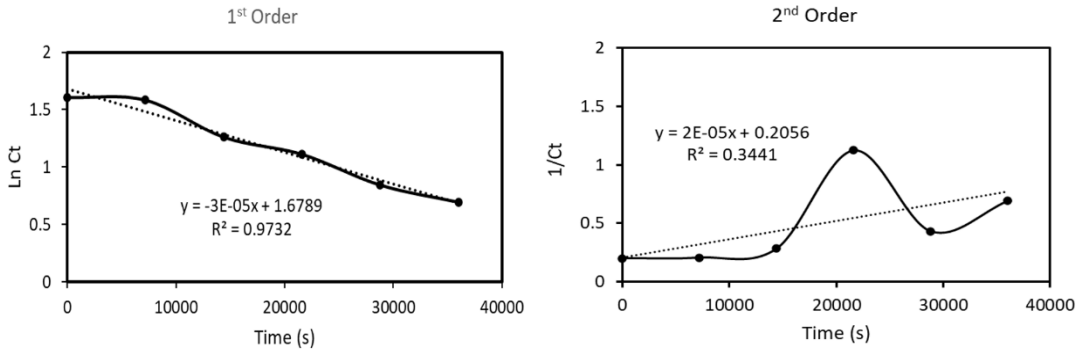

Figure 11. Graph of first and second order reaction equations.

constant as well as the ratio of the reaction rate constants of various samples.

The values of the reaction rate constants for the six samples are shown in Figure 12, where k_{1hours} = 2.76×10^{-5} s^{-1}, k_{2hours} = 2.65×10^{-5} s^{-1}, the k_{3hours} = 2.53×10^{-5} s^{-1}, k_{4hours} = 2.81×10^{-5} s^{-1}, and k_{5hours} = 3.87×10^{-5} s^{-1}. Based on the reaction rate constants (k) obtained, it can be concluded that the bismuth oxide photocatalyst with a calcination time of 5 hours has the best photocatalytic activity. This is supported by the FTIR data where the bismuth oxide with calcination time of 5 hours has the lowest absorption intensity of the Bi-OH group meaning that the number of $Bi(OH)_3$ compounds that were hydrated to Bi_2O_3 is greater than the bismuth oxides calcined with other heating time variations. Additionally, XRD data show that the bismuth oxide with calcination time of 5 hours exhibit tetragonal crystal (-Bi_2O_3) system with the highest amount compared to the other crystalline systems contained. Moreover, the cubic crystal system (β-Bi_2O_3) in the 5 hours calcined Bi_2O_3 is the highest when compared to the other Bi_2O_3. These data are in accordance with the DRS-UV analysis in which bismuth oxide with a calcination time of 5 hours has a band-gap value of 2.49 eV corresponding to the α-Bi_2O_3 band-gap [38]. Data that depict Bi_2O_3 (5 hours) having a higher number of cubic crystal (β-Bi_2O_3) system compared to Bi_2O_3 calcined with other lengths of duration support the fact that Bi_2O_3 (5 hours) has the highest photocatalysis activity. The phenomenon is due to it having a smaller band-gap compared to α-Bi_2O_3. The smaller the band gap value, the better the photocatalysis process will take place since the electrons in the semiconductor are easier to be excited into the conduction band to form holes and electron pairs [39]. Meanwhile, SEM results show that Bi_2O_3 with a calcination time of 5 hours has a small particle size. When a material has a small particle size it has a large surface area. Acers [40] states that a powder sample with a large surface area increases photocatalysis activity.

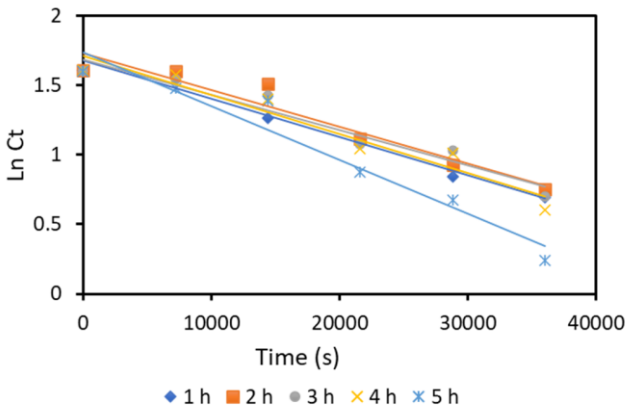

Figure 12. Graph of ln C_t for the value of the reaction rate constant (k) of synthesized bismuth oxide with calcination time variations of 1, 2, 3, 4 and 5 hours.

4. Conclusions

Bismuth oxide has been successfully synthesized using the sol-gel method with calcination time variations of 1, 2, 3, 4, and 5 hours obtaining mass of 2.65, 2.11, 1.88, 1.63 and 1.44 grams each. XRD characterization of samples with calcination times of 1, 2, 3, 4 and 5 hours displays mixed α-Bi_2O_3 and γ-Bi_2O_3 crystal structures. SEM characterization shows the surface of the material appearing gravel like and hollow with a size of about 2-8 µm. FTIR characterization results obtained absorption peaks of 843 cm^{-1} and 1384 cm^{-1} showing the presence of Bi-O-Bi groups. Characterization of DRS-UV-Vis from the best synthesized product obtained a band-gap value of 2.49 eV. TGA characterization was obtained by multi-stage graph type consisting of 12.20% H_2O release (40-140 ° C), 5.33% O_2 release (160-190 °C), and 30.54% N_2 release (220-340 °C). At the temperature of 440 ^{0}C the remaining sample is the stable Bi_2O_3 of 48.07%. The results of photocatalytic activity test showed the percentage of methyl orange degradation with calcination time variations 1, 2, 3, 4, and 5 hours with respective values of 61.12%, 57.74%, 60.01%, 63.66%, 74.93 % and reaction rate constants of 2.76×10^{-5} s^{-1}, 2.65×10^{-5} s^{-1}, 2.53×10^{-5} s^{-1}, 2.81×10^{-5} s^{-1} and 3.87×10^{-5} s^{-1}. Bismuth Oxide with 5 hours calcination time variation has the best photocatalytic activity.

Acknowledgment

The authors gratefully acknowledge the financial support provided by Diponegoro University through the 2023 World Class Research Universitas Diponegoro (WCRU) program, under Grant No. 118-12/UN7.6.1/PP/2021, for the 2023 fiscal year.

CRedit Author Statement

Author Contributions: Author Contributions: Astuti, Y: Conceptualization, Methodology, Investigation, Resources, Data Curation, Writing, Review and Editing, Supervision; Muslim, A: Experiment, Formal Analysis, Data Curation, Writting Draft Preparation; Darmawan, A: Review and Editing, Validation. The authors have read and agreed to the published version of the manuscript.

References

[1] Mallahi, M., Shokuhfar, A., Vaezi, M.R., Esmaeilirad, A., Mazinani, V. (2014). Synthesis and characterization of bismuth oxide nanoparticles via sol-gel method. *American Journal of Engineering Research (AJER)*, 3(4), 162–165.

[2] Sa'adah, F., Sutanto, H., Hadiyanto, H., Hu, C., Liou, Y.S., Ningsih, L.A. (2025). Photodegradation and toxicity assessment of doxycycline using metal (Co, Cu, Fe, and Zn) modified Bi2O3 thin films. *Ceramic International*, 51, 24, 40850-40863. DOI: 10.1016/j.ceramint.2025.06.310.

[3] Sa'adah, F., Sutanto, H. (2022). Optimization of the Bi2O3/Cu synthesis process using response surface methodology as a tetracycline photodegradation agent. *Results in Engineering*, 16, 100521. DOI: 10.1016/j.rineng.2022.100521.

[4] Sa'adah, F., Sutanto, H., Hadiyanto, H., Jaafar, J., Ilsatoham, I., Alkian, I. (2024). Removal of Levofloxacin by Copper Doped Bismuth Oxide Thin Films under UV Light *Irradiation. Journal of Ecological Engineering*, 25(8), 207–221. DOI: 10.12911/22998993/190116.

[5] Khumaeni, A., Jonathan, F., Alkian, I., Sugito, H., Nurhasanah, I., Ibrahim, R.K.R., Julkapli, N.M. (2025). Direct synthesis of bismuth-doped ZnO nanoparticles in liquid precursor: A one-step pulsed laser ablation approach for enhanced photocatalytic dye removal. *Journal of Molecular Liquids*, 128054. DOI: 10.1016/j.molliq.2025.128054.

[6] Pandiangan, I.F.D., Sutanto, H., Nurhasanah, I. (2018). Effect of annealing temperature on optical properties and photocatalytic properties of TiO2: N 8% thin film for rhodamine B degradation. *Materials Research Express*, 5(8), 086404. DOI: 10.1088/2053-1591/aad15d.

[7] Ariyanti, D., Mills, L., Dong, J., Yao, Y., Gao, W. (2017). NaBH4 modified TiO2: Defect site enhancement related to its photocatalytic activity. *Materials Chemistry and Physics*, 199, 571–576. DOI: 10.1016/j.matchemphys.2017.07.054.

[8] Sutanto, H., Wibowo, S., Hidayanto, E., Nurhasanah, I., Hadiyanto, H. (2015). Synthesized of Double Layer Thin Film ZnO/ZnO: Ag by Sol-Gel Method for Direct Blue 71 Photodegradation. *Reaktor*, 15(3), 175–181. DOI: 10.14710/reaktor.15.3.175-181.

[9] Kusworo, T.D., Azizah, D.A., Kumoro, A.C., Kurniawan, T.A., Othman, M.H.D. (2023). Fabrication, characterization, and application of PSf/Ni@ ZnO amalgamated membrane for photocatalytic degradation of dyeing wastewater from batik industry. *Materials Today Chemistry*, 30, 101493. DOI: 10.1016/j.mtchem.2023.101493

[10] Qiu, Y., Yang, M., Fan, H., Zuo, Y., Shao, Y., Xu, Y., Yang, X., Yang, S. (2011). Phase-transitions of α-and ß-Bi2O3 nanowires. *Materials Letters*, 65(4), 780–782. DOI: 10.1016/j.matlet.2010.11.045.

[11] Hernandez-Delgadillo, R., Velasco-Arias, D., Martinez-Sanmiguel, J.J., Diaz, D., Zumeta-Dube, I., Arevalo-Niño, K., Cabral-Romero, C. (2013). Bismuth oxide aqueous colloidal nanoparticles inhibit Candida albicans growth and biofilm formation. *International Journal of Nanomedicine*, 8(1), 1645–1652. DOI: 10.2147/IJN.S38708.

[12] Astuti, Y., Fauziyah, A., Nurhayati, S., Wulansari, A.D., Andianingrum, R., Hakim, A.R., Bhaduri, G. (2016). Synthesis of α-Bismuth oxide using solution combustion method and its photocatalytic properties. In: *IOP Conference Series: Materials Science and Engineering*. IOP Publishing, p. 012006. DOI: 10.1088/1757-899X/107/1/012006.

[13] La, J., Huang, Y., Luo, G., Lai, J., Liu, C., Chu, G. (2013). Synthesis of bismuth oxide nanoparticles by solution combustion method. *Particulate Science and Technology*, 31(3), 287–290. DOI: 10.1080/02726351.2012.727525.

[14] Astuti, Y., Amri, D., Widodo, D.S., Widiyandari, H., Balgis, R., Ogi, T. (2020). Effect of fuels on the physicochemical properties and photocatalytic activity of bismuth oxide, synthesized using solution combustion method. *International Journal of Technology*, 11(1), 26-36. DOI: 10.14716/ijtech.v11i1.3342.

[15] Astuti, Y., Elesta, P.P., Widodo, D.S., Widiyandari, H., Balgis, R. (2020). Hydrazine and urea fueled-solution combustion method for Bi2O3 synthesis: characterization of physicochemical properties and photocatalytic activity. *Bulletin of Chemical Reaction Engineering & Catalysis*, 15(1), 104–111. DOI: 10.9767/bcrec.15.1.5483.104-111.

[16] Astuti, Y., Mulyana, T.N., Tasiman, B.H.A., Darmawan, A., Widyandari, H. (2023). Hydrazine-fueled solution combustion method: Fuel/oxidizer ratio effects on photocatalytic performance of bismuth oxide. *Bulletin of Chemical Reaction Engineering & Catalysis*, 18(3), 539–547. DOI: 10.9767/bcrec.19943.

[17] Anilkumar, M., Pasricha, R., Ravi, V. (2005). Synthesis of bismuth oxide nanoparticles by citrate gel method. *Ceramics International*, 31(6), 889–891. DOI: 10.1016/j.ceramint.2004.09.002.

[18] Yang, Q., L.Y.W., Y.Q., W.P.-L.L., & C.Y.B. (2002). Hydrothermal Synthesis of Bismuth Oxide Needles. *Materials Letters*, 55(1–2), 46–49. DOI: 10.1016/S0167-577X(01)00617-6.

[19] Amiri, A. (2016). Solid-phase microextraction-based sol–gel technique. *TrAC Trends in Analytical Chemistry*, 75, 57–74. DOI: 10.1016/j.trac.2015.10.003.

[20] Pinjari, D. V, Prasad, K., Gogate, P.R., Mhaske, S.T., Pandit, A.B. (2015). Synthesis of titanium dioxide by ultrasound assisted sol–gel technique: Effect of calcination and sonication time. *Ultrasonics Sonochemistry*, 23, 185–191. DOI: 10.1016/j.ultsonch.2014.10.017.

[21] Weidong, H., Wei, Q., Xiaohong, W., Xianbo, D., Long, C., Zhaohua, J. (2007). The photocatalytic properties of bismuth oxide films prepared through the sol–gel method. *Thin Solid Films*, 515(13), 5362–5365. DOI: 10.1016/j.tsf.2007.01.031.

[22] Astuti, Y., Listyani, B.M., Suyati, L., Darmawan, A. (2021). Bismuth oxide prepared by sol-gel method: variation of physicochemical characteristics and photocatalytic activity due to difference in calcination temperature. *Indonesian Journal of Chemistry*, 21(1), 108–117. DOI: 10.22146/ijc.53144.

[23] Ilsatoham, M.I., Alkian, I., Azzahra, G., Hidayanto, E., Sutanto, H. (2023). Effect of substrate temperature on the properties of Bi2O3 thin films grown by sol-gel spray coating. *Results in Engineering*, 17, 100991. DOI: 10.1016/j.rineng.2023.100991.

[24] Kusworo, T.D., Kumoro, A.C., Aryanti, N., Kurniawan, T.A., Dalanta, F., Alias, N.H. (2023). Photocatalytic polysulfone membrane incorporated by ZnO-MnO2@ SiO2 composite under UV light irradiation for the reliable treatment of natural rubber-laden wastewater. *Chemical Engineering Journal*, 451, 138593. DOI: 10.1016/j.cej.2022.138593.

[25] Astuti, Y., Nurhayati, S., Arnelli (2022). Effect of calcination temperature on the morphology and photocatalytic activity of Bismuth oxide. In: *AIP Conference Proceedings*. AIP Publishing LLC, p. 020043. DOI: 10.1063/5.0104124.

[26] Hwang, B.J., Santhanam, R., Liu, D.G., Tsai, Y.W. (2001). Effect of Al-substitution on the stability of LiMn2O4 spinel, synthesized by citric acid sol–gel method. *Journal of Power Sources*, 102(1–2), 326–331. DOI: 10.1016/S0378-7753(01)00657-7.

[27] Eastaugh, N., Walsh, V., Chaplin, T., Siddall, R. (2007). Pigment compendium: a dictionary of historical pigments. Routledge.

[28] Bartonickova, E., Cihlar, J., Castkova, K. (2007). Microwave-assisted synthesis of bismuth oxide. *Processing and Application of Ceramics*, 1(1–2), 29–33. DOI: 10.2298/PAC0702029B.

[29] Bandyopadhyay, S., Dutta, A. (2017). Thermal, optical and dielectric properties of phase stabilized δ–Dy-Bi2O3 ionic conductors. *Journal of Physics and Chemistry of Solids*, 102, 12–20. DOI: 10.1016/j.jpcs.2016.11.001.

[30] Abdullah, E.A., Abdullah, A.H., Zainal, Z., Hussein, M.Z., Ban, T.K. (2012). Synthesis and Characterisation of Penta-Bismuth Hepta-Oxide Nitrate, Bi5O7NO3, as a New Adsorbent for Methyl Orange Removal from an Aqueous Solution. *Journal of Chemistry*, 9(4), 2429–2438. DOI: 10.1155/2012/707853.

[31] Daniyati, R., Zharvan, V., Ichsan, N., Pramono, Y.H., Yudoyono, G. (2015). Penentuan energi celah pita optik film TiO2 menggunakan metode tauc plot. In: *Prosiding Seminar Sains dan Teknologi*. p. 5329. DOI: 10.3390/su14084500.

[32] Iyyapushpam, S., Nishanthi, S.T., Padiyan, D.P. (2014). Enhanced photocatalytic degradation of methyl orange by gamma Bi2O3 and its kinetics. *Journal of Alloys and Compounds*, 601, 85–87. DOI: 10.1016/j.jallcom.2014.02.142.

[33] Ibhadon, A.O., Fitzpatrick, P. (2013). Heterogeneous photocatalysis: recent advances and applications. *Catalysts*, 3(1), 189–218. DOI: 10.3390/catal3010189.

[34] Devi, L.G., Kumar, S.G., Reddy, K.M., Munikrishnappa, C. (2009). Photo degradation of Methyl Orange an azo dye by Advanced Fenton Process using zero valent metallic iron: Influence of various reaction parameters and its degradation mechanism. *Journal of Hazardous Materials*, 164(2–3), 459–467. DOI: 10.1016/j.jhazmat.2008.08.017.

[35] Radini, I.A., Hasan, N., Malik, M.A., Khan, Z. (2018). Biosynthesis of iron nanoparticles using Trigonella foenum-graecum seed extract for photocatalytic methyl orange dye degradation and antibacterial applications. *Journal of Photochemistry and Photobiology B: Biology*, 183, 154–163. DOI: 10.1016/j.jphotobiol.2018.04.014.

[36] Liu, X., Deng, H., Yao, W., Jiang, Q., Shen, J. (2015). Preparation and photocatalytic activity of Y-doped Bi2O3. *Journal of Alloys and Compounds*, 651, 135–142. DOI: 10.1016/j.jallcom.2015.08.068.

[37] Wang, Q., Hui, J., Yang, L., Huang, H., Cai, Y., Yin, S., Ding, Y. (2014). Enhanced photocatalytic performance of Bi2O3/H-ZSM-5 composite for rhodamine B degradation under UV light irradiation. *Applied Surface Science*, 289, 224–229. DOI: 10.1016/j.apsusc.2013.10.139.

[38] Bedoya Hincapie, C.M., Pinzon Cardenas, M.J., Alfonso Orjuela, J.E., Restrepo Parra, E., Olaya Florez, J.J. (2012). Physical-chemical properties of bismuth and bismuth oxides: Synthesis, characterization and applications. *Dyna*, 79(176), 139–148.

[39] Rahmadhani, D., Ratnawulan, R., Hidayati, H., Fauzi, A., Steven, A., Azleen, F. (2023). Effect of Temperature Variation on Band Gap Value in Thin Layers of Nano Photocatalyst Fe2O3/CuO/MnO2. In: *Journal of Physics: Conference Series*. IOP Publishing, p. 012036. DOI: 10.1088/1742-6596/2582/1/012036.

[40] Acers (2010). Progress in Nanotechnology: Processing. Wiley.